FIBRE AND INTEGRATED OPTICS

PACS numbers: 42.81.Dp; 42.65.Sf
DOI: 10.1070/QE2009v039n08ABEH014011

Modulation instability of narrow-band nanosecond pulses propagating in anomalous-dispersion fibre

A.E. Ismagulov, S.A. Babin, E.V. Podivilov, M.P. Fedoruk, I.S. Shelemba, O.V. Shtyrina

***Abstract*. We demonstrate that, in the presence of noise, propagation of narrow-band 100-ns pulses through a 6-km long optical fibre sharply reduces their amplitude when a threshold power (~ 0.2 W) is exceeded. The effect is due to the development of modulation instability and is sensitive to the noise level in the spectral region ~ 100 GHz in width around the central frequency.**

Keywords: *modulation instability, nanosecond pulse, narrow-band fibre laser*.

1. Introduction

Recent years have seen rapid progress in the development of distributed optical fibre measuring systems that utilise pulsed narrow-band probe radiation sources [1, 2], in particular of Brillouin-based temperature sensors [3, 4], time-division-multiplexed fibre Bragg grating temperature sensor arrays [5] and phase-sensitive Rayleigh OTDR intrusion sensor systems [6, 7].

The radiation source in such systems is typically a laser with a wavelength within the transmission window of the fibre ($\lambda \approx 1.55$ μm) and a pulse duration $\tau \sim 100$ ns, which ensures a spatial resolution of ~ 10 m.

When a single longitudinal mode of the laser is selected (single-frequency regime), the width of its emission spectrum is determined by the pulse duration ($\Delta\nu \simeq 11.6$ MHz at ~ 100 ns). To achieve high pulse powers (at least 1 W), use is commonly made of (semiconductor) master oscillator/(erbium-doped fibre) power amplifier configurations. The output spectrum then contains, in addition to pulses, a noise continuum due to the amplified spontaneous emission of the erbium amplifier.

The purpose of this work is to study the nonlinear effects that accompany the propagation of such pulses in a long optical fibre, in particular, the power limitations resulting from modulation instability (MI). Note that MI is well studied for picosecond pulses [8], whereas in the case of nanosecond pulses only MI-induced changes in the amplitude of the Brillouin scattering signal have been described [9]. The study of MI effects on the propagation of nanosecond pulses in the presence of noise is of current interest for both understanding the physics of the process and clarifying the limitations that the properties of the radiation source impose on the parameters of distributed sensor systems [1 – 7, 9].

2. Experimental

The source used (Fig. 1) is similar to that described by Gorshkov et al. [7]. The radiation from pulsed laser diode (*1*) frequency-stabilised by an external Bragg grating is sent to two-stage erbium amplifier (*3*) and then coupled into a 6-km-long section of single-mode fibre (*5*). The length of the active fibre is $L_1 = 2$ m in the first amplifier and $L_2 = 6$ m in the second amplifier. The amplifiers are pumped by 980-nm laser diodes (*2*). The pump power is 30 mW for the first amplifier and is varied from zero to 40 mW for the second. The Bragg gratings (*4*) ensure spectral filtration of the signal around ~ 1550 nm. The light pulses are bell-shaped, with a full width at half maximum (FWHM) of ~ 100 ns and a repetition rate of ~ 0.5 kHz (Fig. 2).

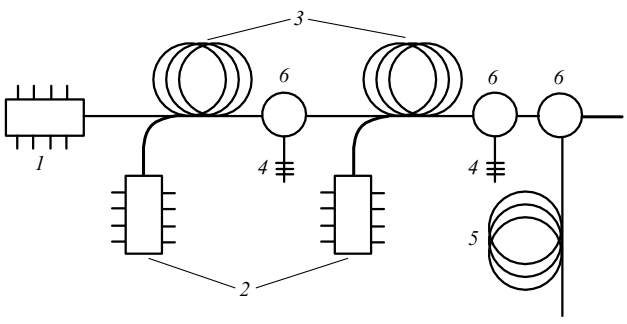

Figure 1. Schematic of the experimental setup: (*1*) pulsed laser diode; (*2*) pump laser diodes; (*3*) active erbium fibres; (*4*) Bragg grating filters; (*5*) 6 km of passive single-mode fibre; (*6*) fibre circulators.

A.E. Ismagulov, I.S. Shelemba Institute of Automation and Electrometry, Siberian Branch, Russian Academy of Sciences, prosp. Akad. Koptyuga 1, 630090 Novosibirsk, Russia; e-mail: arsen.ismagulov@gmail.com;
S.A. Babin, E.V. Podivilov Institute of Automation and Electrometry, Siberian Branch, Russian Academy of Sciences, prosp. Akad. Koptyuga 1, 630090 Novosibirsk, Russia; Novosibirsk State University, ul. Pirogova 2, 630090 Novosibirsk, Russia; e-mail: babin@iae.nsk.su;
M.P. Fedoruk Institute of Computational Technologies, Siberian Branch, Russian Academy of Sciences, prosp. Akad. Lavrent'eva 6, 630090 Novosibirsk, Russia; Novosibirsk State University, ul. Pirogova 2, 630090 Novosibirsk, Russia; e-mail: mife@ict.nsk.ru;
O.V. Shtyrina Institute of Computational Technologies, Siberian Branch, Russian Academy of Sciences, prosp. Akad. Lavrent'eva 6, 630090 Novosibirsk, Russia; e-mail: olya.shtyrina@gmail.com

Received 24 November 2008; revision received 15 April 2009
Kvantovaya Elektronika **39** (8) 765 – 769 (2009)
Translated by O.M. Tsarev

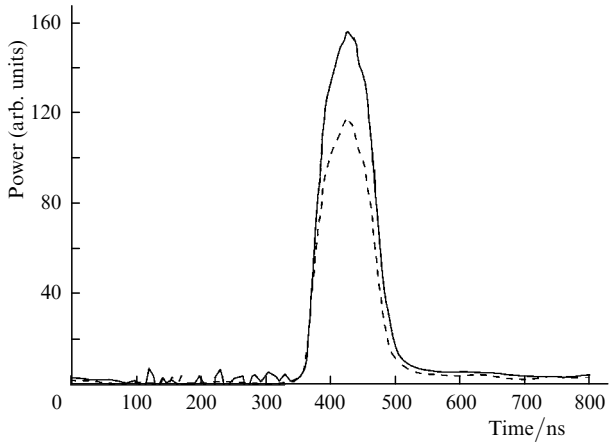

Figure 2. Observed pulse shapes of the input signal (solid line) and at the 6-km fibre output (dashed line).

We measured the time-averaged spectrum and average power of the input signal and those at the 6-km fibre output. The pulse shape showed no significant changes after 6-km transmission (Fig. 2).

Figure 3 shows the input spectra at different pump powers and the corresponding emission spectra at the output of the long fibre. The pulse consists of a narrow peak with a width of ~ 0.01 nm (~ 1 GHz), determined by the resolution of the spectrum analyser, and a broad (~ 1 nm) noise band, determined by the spectral width of the Bragg grating filter that cuts off the amplifier spontaneous emission noise. Relative to the spectral density of the peak, the noise level is of the order of -15 dB within the band and about -45 dB outside it. Note that the actual width of the peak is two to three orders of magnitude smaller than that measured by the spectrum analyser and, accordingly, the relative noise level is about 25 dB lower.

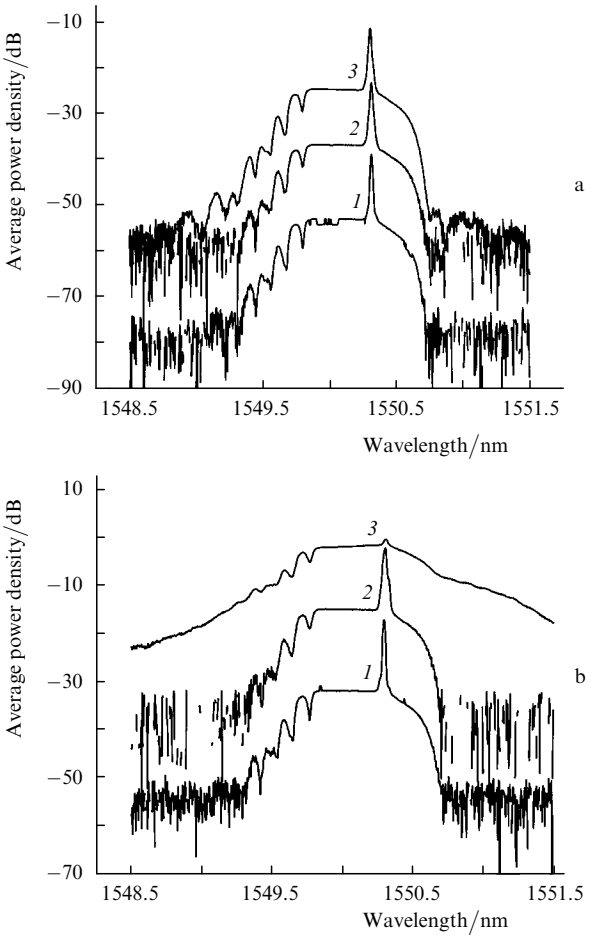

Figure 3. (a) Input and (b) output spectra at average input powers $P = 0.13$ (*1*), 12 (*2*) and 204 μW (*3*).

Analysis of the emission spectra indicates that, at high input powers, the output peak height decreases, the relative amplitude of the noise pedestal rises, and its spectrum broadens. The average output power is then a linear function of the average input power, with the standard relation $\overline{P(L)} = \overline{P(0)}e^{-\alpha L}$, where $\alpha = 0.17$ dB km^{-1} is the measured loss in the fibre.

To assess the behaviour of the peak power, the measured input spectra were decomposed into narrow (peak) and broad (pedestal) components. In the input spectra, the narrow component corresponds to the light pulse, and the broad component, to a noise continuum. The integrals of these components over the spectrum and time correspond to their average powers.

At the fibre output, we observe a narrow peak and a pedestal, the latter consisting of a continuous component and an impulsive component (which is assumed to result from power transfer to the pedestal because of the MI effect).

To find the actual peak and pedestal powers, we solved a set of linear equations, assuming that the continuous component of noise experiences only absorption in the fibre. The output power versus input power, $P_{\text{out}}(P_{\text{in}})$, data thus obtained for the narrow and broad components (Fig. 4) show clearly that pulse propagation in the fibre is accompanied by power transfer from the narrow peak to the broad noise pedestal.

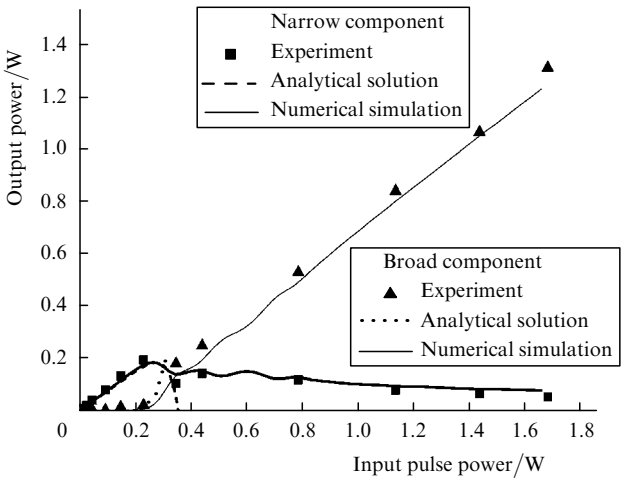

Figure 4. Output power vs. input pulse power for the narrow and broad components of the pulse.

3. Analytical model

The propagation of a long pulse in an optical fibre can be described by the nonlinear Schrödinger equation (NSE)

$$\frac{\partial A}{\partial z} + \frac{1}{c}\frac{\partial A}{\partial t} = i\frac{|\beta_2|}{2}\frac{\partial^2}{\partial t^2}A + i\gamma|A|^2A - \alpha A, \qquad (1)$$

where $A(t,z)$ is the amplitude of the electromagnetic field at the carrier frequency $\omega_0 = 2\pi n_0/\lambda_0$, normalised to the power $P = |A|^2$; c is the speed of light in the fibre with a refractive index n_0; $\beta_2 = -10\ \mathrm{km^{-1}\ nm^{-2}}$ is the (anomalous) dispersion at a wavelength of 1550 nm; $\gamma = 3\ \mathrm{W^{-1}\ km^{-1}}$ is the nonlinearity coefficient; and $\alpha = 0.17\ \mathrm{dB\ km^{-1}}$ is the optical loss coefficient. The boundary condition at the fibre input, $z = 0$, is expressed as the sum of a Gaussian pulse shape with a FWHM $T_0 = 100$ ns and the noise amplitude $A_\mathrm{n}(t)$:

$$A(t,0) = \sqrt{P_0}\exp\left(-\frac{t^2}{T_0^2}2\ln 2\right)\sqrt{\frac{4\ln 2}{\pi}} + A_\mathrm{n}(t). \qquad (2)$$

Here, $P_0 = \varepsilon_0/T_0$ is the average power of a pulse of energy ε_0. The random noise has a power spectral density $P_\mathrm{n}(\omega) = |A_\mathrm{n}(\omega)|^2$ that differs from zero ($\overline{P_\mathrm{n}(\omega)} = \varepsilon_\mathrm{n}/\Delta$) in the spectral range $\Delta = 1$ nm around the carrier frequency ω_0, ε_n is the noise energy averaged over the pulse period, $\tau = 2$ ms. The measured pulse-to-noise energy ratio is $\varepsilon_0/\varepsilon_\mathrm{n} = 0.71$.

In a fibre with an anomalous group velocity dispersion, a pulse breaks up because of MI. To describe this effect, we divide the time axis into segments of length $\delta T \ll T_0$ such that $P(t_i)$ can be considered constant within each segment. Neglecting the influence of the noise component, we obtain for the pulse amplitude in each segment

$$A_\mathrm{p}^{(i)}(z) = A_\mathrm{p}(t_i,0)\exp(\mathrm{i}\gamma P_i z - \alpha z), \qquad (3)$$

where $P_i = |A_\mathrm{p}^{(i)}|$.

Consider the case $\alpha L \ll 1$, where losses can be neglected. We obtain the following equations for the noise component in the ith segment in the spectral representation:

$$\frac{\mathrm{d}A_\mathrm{n}^{(i)}(\omega)}{\mathrm{d}z} = \left(-\mathrm{i}\frac{|\beta|}{2}\omega^2 + 2\mathrm{i}\gamma P_i\right)A_\mathrm{n}^{(i)}(\omega) + \mathrm{i}\gamma A_\mathrm{p}^{(i)2}(z)A_\mathrm{n}^{(i)*}(\omega), \qquad (4)$$

$$\frac{\mathrm{d}A_\mathrm{n}^{(i)*}(\omega)}{\mathrm{d}z} = \left(\mathrm{i}\frac{|\beta|}{2}\omega^2 - 2\mathrm{i}\gamma P_i\right)A_\mathrm{n}^{(i)*}(\omega) - \mathrm{i}\gamma A_\mathrm{p}^{(i)*2}(z)A_\mathrm{n}^{(i)}(\omega). \qquad (5)$$

Seeking the solution to this linear equation in the form $A_\mathrm{n}^{(i)}(\omega)\exp(\mathrm{i}\gamma P_i z + vz)$, we obtain an algebraic equation for v,

$$v_i^2 + \left(\gamma P_i - \frac{|\beta|}{2}\omega^2\right)^2 - (\gamma P_i)^2 = 0. \qquad (6)$$

Therefore,

$$v_\pm = \pm\left[\left(2\gamma P_i - \frac{|\beta|}{2}\omega^2\right)\frac{|\beta|\omega^2}{2}\right]^{1/2}. \qquad (7)$$

The solutions with v_+ rise exponentially starting at the noise level $\overline{P_\mathrm{n}^i(\omega)} = \varepsilon_\mathrm{n}\delta T/\Delta T$:

$$P_\mathrm{n}^{(i)}(\omega,z) = P_\mathrm{n}^{(i)}(\omega)\exp[2v_+(\omega)z]. \qquad (8)$$

The components that grow most rapidly are those with frequencies $\omega_\mathrm{MI} = \pm\sqrt{2\gamma P_i/|\beta|}$ and with $v_+^{(i)} = \gamma P_i$, proportional to the pulse power in the ith segment.

The noise grows exponentially until its energy, $\int_\omega P_\mathrm{n}^{(i)}(\omega,z)\mathrm{d}\omega$, becomes equal to the pulse energy in the ith segment, after which the reverse influence of the noise on the pulse must be taken into account:

$$P_\mathrm{n}^{(i)}(z) = \int\frac{\mathrm{d}\omega}{2\pi}P_\mathrm{n}^{(i)}(\omega,z) \simeq \frac{\varepsilon_\mathrm{n}\delta T}{\Delta\tau} \times \int\frac{\mathrm{d}\omega}{2\pi}\exp\left\{2z\left[\left(2\gamma P_i - \frac{|\beta|}{2}\omega^2\right)\frac{|\beta|\omega^2}{2}\right]^{1/2}\right\}. \qquad (9)$$

For $4\gamma P_i z \gg 1$, this integral can be estimated by Laplace's method. The major contribution comes from the two maxima at $\omega_\mathrm{MI} = \pm\sqrt{2\gamma P_i/|\beta|}$:

$$P_\mathrm{n}^{(i)}(L) = \varepsilon_\mathrm{n}\frac{\delta T}{\Delta\tau}\exp(2\gamma P_i L)\left(\frac{1}{4\pi|\beta|L}\right)^{1/2}. \qquad (10)$$

Note that, outside the pulse at $|t| \ll T_0$, the noise amplitude does not grow because there is no coupling with the pulse. For this reason, the noise energy over the pulse period comprises two contributions:

$$\varepsilon_\mathrm{n}(L) = \sum_i P_\mathrm{n}^{(i)}(L) = \varepsilon_\mathrm{n} + \frac{\varepsilon_\mathrm{n}}{(4\pi|\beta|\Delta^2 L)^{1/2}}\int_{-T_0}^{T_0}\exp(2\gamma LP(t))\frac{\mathrm{d}t}{\tau}. \qquad (11)$$

The integral above can also be estimated by Laplace's method to give the noise energy in the pulse position, $\varepsilon_\mathrm{n}^\mathrm{p}(L)$. The average noise power at the fibre output comprises a continuous component, $\bar{P}_\mathrm{n} = \varepsilon_\mathrm{n}/\tau$, and an impulsive component,

$$\bar{P}_\mathrm{n}^\mathrm{p} = \frac{\varepsilon_\mathrm{n}^\mathrm{p}}{\tau} = \frac{T_0}{\tau}\frac{\varepsilon_\mathrm{n}}{\tau}\frac{\sqrt{\pi}\exp[8\gamma LP_0\ln(2)/\pi]}{[64|\beta|\Delta^2L^2\gamma P_0(\ln 2)^2]^{1/2}}. \qquad (12)$$

These solutions are valid as long as the regular pulse energy, $\varepsilon_0 = P_0T_0$, far exceeds the energy of the noise component, $\varepsilon_\mathrm{n}^\mathrm{p}(L)$:

$$\frac{\varepsilon_0}{\varepsilon_\mathrm{n}} = 0.71 \gg \frac{T_0}{\tau}\frac{\sqrt{\pi}\exp[8\gamma LP_0\ln(2)/\pi]}{[64|\beta|\Delta^2L^2\gamma P_0(\ln 2)^2]^{1/2}}. \qquad (13)$$

The dashed and dotted lines in Fig. 4 illustrate the behaviour of the noise power calculated by Eqn (12) and that of the power of the narrow component, $P_\mathrm{p}(L)$, evaluated from the conservation-of-energy principle:

$$P_\mathrm{p}(L) = P_0 - \overline{P_\mathrm{n}^\mathrm{p}(L)}\tau/T_0. \qquad (14)$$

4. Numerical simulation

Since the analytical solution is valid only near the MI threshold, numerical simulation is needed at higher powers.

To numerically solve Eqn (1), we used the process splitting method, in which the solution to Eqn (1) at a step Δz of an evolution variable can be represented in the form

$$A(z+\Delta z,t) = \exp(\tfrac{1}{2}\Delta z\widetilde{N})\exp(\Delta z\widetilde{D})\exp(\tfrac{1}{2}\Delta z\widetilde{N})A(z,t), \qquad (15)$$

where $\widetilde{N}$ is a nonlinear operator and $\widetilde{D}$ is a linear operator that takes into account the dispersion broadening and attenuation of the pulse. In our simulations, the time window was $T = 1$ μs, and the number of time steps was $N = 2^{20}$. The step of the evolution variable was $\Delta z = 5$ m. The initial distribution had the form of a Gaussian pulse with a FWHM of 100 ns and a varied peak power P_p. Thus, the field distribution at the fibre input was

$$A(t,0) = \sqrt{P_p}\exp(-t^2/2T_0^2)$$

with white Gaussian noise in a 1-nm spectral band. The simulation results are represented in Fig. 4 by solid lines. Figure 5 shows the intensity as a function of time at the fibre input and after 6-km propagation for a peak pulse power $P_p = 1.3$ W. The development of MI leads to strong modulation of the pulse amplitude at the fibre output, with a characteristic period $T_{MI} \sim 10$ ps (with spikes an order of magnitude above the average level).

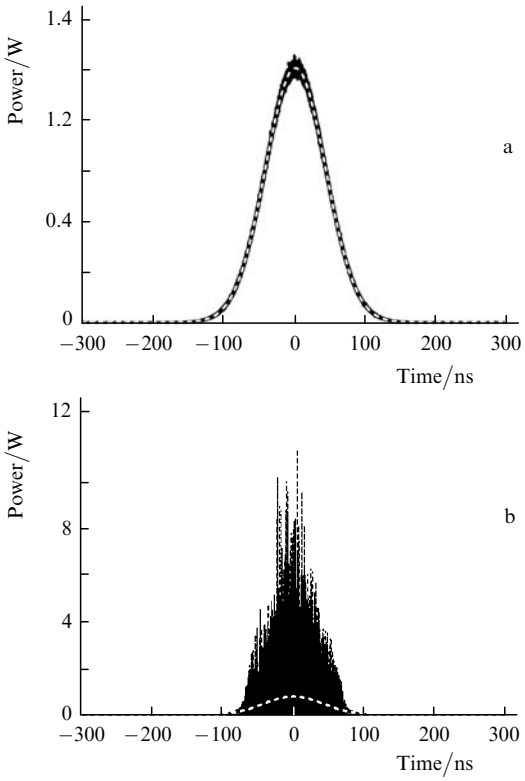

Figure 5. (a) Initial pulse shape in the simulation and (b) simulated pulse shape at the 6-km fibre output. The white dashed line shows the pulse envelope.

5. Discussion

Our experimental data indicate that, in the presence of broadband noise, the power of the transmitted narrow-band radiation first rises linearly with input power, then saturates at some threshold value and falls off at higher input powers (Fig. 4). Because of the MI effect, the power of the narrow peak is transferred to the noise pedestal, whose intensity rises linearly at high powers.

As seen in Fig. 4, our analytical model provides a sufficiently accurate prediction of the threshold input pulse power, P_{th}^{p}, above which the transmitted power of the peak decreases. The threshold power can be found by putting an equal sign in (13):

$$P_{th}^{p} = \frac{\pi}{8\gamma L \ln 2}\ln\left\{\frac{\varepsilon_0}{\varepsilon_n}\frac{\tau}{T_0}[64|\beta|\Delta^2 L^2\gamma P_0(\ln 2)^2/\pi)]^{1/2}\right\}. \quad (16)$$

The actual loss in a 6-km fibre at the threshold pulse power is $e^{-\alpha L} \sim 0.8$. Since the above analytical model assumes that $\alpha L \ll 1$, the threshold power for MI is slightly underestimated, but by no more than 20 %.

In the above expression, P_{th}^{p} is inversely proportional to the fibre length and is a logarithmic function of noise spectral density ε_n in the frequency range $\omega_{MI} = \pm\sqrt{2\gamma P_i/|\beta|}$. Therefore, the threshold for MI can be raised by reducing the noise level in the ω_{MI} range. At the pulse powers used in our experiments (~ 1 W), the width of the spectral range corresponding to ω_{MI} is $\Delta\lambda \simeq 1$ nm. Thus, the continuous noise spectrum falls in this range, leading to strong energy transfer from the narrow peak to the broad pedestal.

One way to suppress MI is to reduce the noise level. In particular, in a study reported by Alahbabi et al. [9] the noise level measured by a spectrum analyser was 25 dB lower than that in this study, and no reduction in the amplitude of the narrow peak was detected. At an input power of ~ 0.4 W, small sidebands emerged in the spectrum because of the MI effect, affecting the characteristics of the frequency-shifted SBS signal. Alahbabi et al. [9] showed that, in a dispersion-shifted fibre (normal-dispersion regime at 1550 nm), no MI developed. The same would be expected in our case.

The curve obtained by numerical simulation agrees both qualitatively and quantitatively with the experimental data, even in details such as peak power oscillations in the falloff region.

The numerical simulation also suggests that the pulse envelope remains undistorted, but the pulse at the output end of the long fibre is heavily modulated (Fig. 5) at a frequency of ~ 100 GHz. Indeed, the pulse shape remains unchanged in our experiments, but no spikes can be detected because of the time averaging in the measuring channel ($\sim$ 100-MHz frequency band).

6. Conclusions

The present results demonstrate that, when a certain power level is exceeded, propagation through a long ($\sim$ 6km) optical fibre sharply reduces the amplitude of narrow-band 100-ns pulses because of the development of MI, which leads to energy transfer to spectral sidebands.

The MI threshold is inversely proportional to the fibre length ($P_{th}^{p} \approx 0.2$ W at $L = 6$ km) and falls off logarithmically with noise power spectral density in the frequency range ~ 1 nm in width around the carrier frequency.

MI may have a significant effect on the performance of phase-sensitive Rayleigh sensor systems that utilise Rayleigh scattering [7]. Its role can be reduced by decreasing the noise component of the input signal or passing to the normal-dispersion regime of the fibre.

Acknowledgements. This work was supported by the Siberian Division of the Russian Academy of Sciences through an integrated research project and by a grant from the RF Ministry of Education and Science.

References

1. Barnoski M.K., Rourke M.D., Jensen S.M., Melville R.T. *Appl. Opt*., **16**, 2375 (1977).
2. Healey P. *J. Lightwave Technol*., **LT-3**, 876 (1985).
3. Bao X., Webb D.J., Jackson D.A. *Opt. Lett*., **19**, 141 (1994).
4. Horiguchi T., Shimizu K., Kurashima T., Tateda M., Koyamada Y. *J. Lightwave Technol*., **13**, 1296 (1995).
5. Wilson A., James S.W., Tatam R.P. *Opt. Fiber Sensors*, **16**, 475 (1997).
6. Juarez J.C., Maier E.W., Choi K.N., Taylor H.F. *J. Lightwave Technol*., **23**, 2081 (2005).
7. Gorshkov B.G., Paramonov V.M., Kurkov A.S., Kulakov A.T., Zazirnyi M.V. *Kvantovaya Elektron*., **36**, 963 (2006) [*Quantum Electron*., **36**, 963 (2006)].
8. Tai K., Hasegawa A., Tomita A. *Phys. Rev. Lett*., **56**, 135 (1986).
9. Alahbabi M.N., Cho Y.T., Newson T.P., Wait P.C., Hartog A.H. *J. Opt. Soc. Am. B*, **21**, 1156 (2004).